**Earth, Planets and Space**

## EXPRESS LETTER

**Open Access**

CrossMark

# San-in shear zone in southwest Japan, revealed by GNSS observations

Takuya Nishimura[1*] and Youichiro Takada[2]

## Abstract

A right-lateral shear zone in the San-in region, southwest Japan, has been proposed by previous geological and seismological studies. It locates 350 km north of the Nankai Trough, that is, the main plate boundary between the subducting Philippine Sea and overriding Amurian plates and presumably accommodates a part of the relative plate motion. We present a geodetic evidence of the proposed shear zone using GNSS velocity data. Distinct shear deformation is identified only between ~132.5°E and ~135°E along a coastline which is a part of the proposed shear zone, and we propose to call the geodetically identified shear zone as the San-in shear zone (SSZ). The SSZ is a concentrated deformation zone with a width of ~50 km and can be modeled by a deep creep on a vertical strike slip fault with a creep rate of ~5 mm/year. There are some active faults parallel and oblique to the overall trend of the SSZ, but no single active fault coincides with the SSZ. Lineaments of microseismicity and source faults of large earthquakes are almost oriented in NNW–SSE in the SSZ and oblique to the overall trend of the SSZ. They are interpreted as conjugate Riedel shears. Based on these geodetic, seismological, and geomorphological observations, we suggest that the SSZ is a developing and young shear zone in a geological time scale.

**Keywords:** San-in shear zone (SSZ), Strain concentration zone, GNSS, Southwest Japan

## Introduction

Southwest Japan is situated in the subduction zone where the Philippine Sea plate subducts from the Nankai Trough. Previous studies proposed that some tectonic structures in the southeastern margin of the overriding Amurian plate (i.e., southwest Japan) developed as a result of strain partitioning in response to the oblique subduction of the Philippine Sea plate (e.g., Tsukuda 1992; Gutscher and Lallemand 1999; Itoh et al. 2002) (Fig. 1). One of the most important structures is the Median Tectonic Line, 200 km north of the Nankai Trough. The other is the Northern Chugoku shear zone (NCSZ) (Gutscher and Lallemand 1999) or the Southern Japan Sea Strike Slip Fault Zone (SJSFZ) (Itoh et al. 2002), 350 km north of the Nankai Trough. They are presumably right-lateral strike slip fault zones in the San-in region

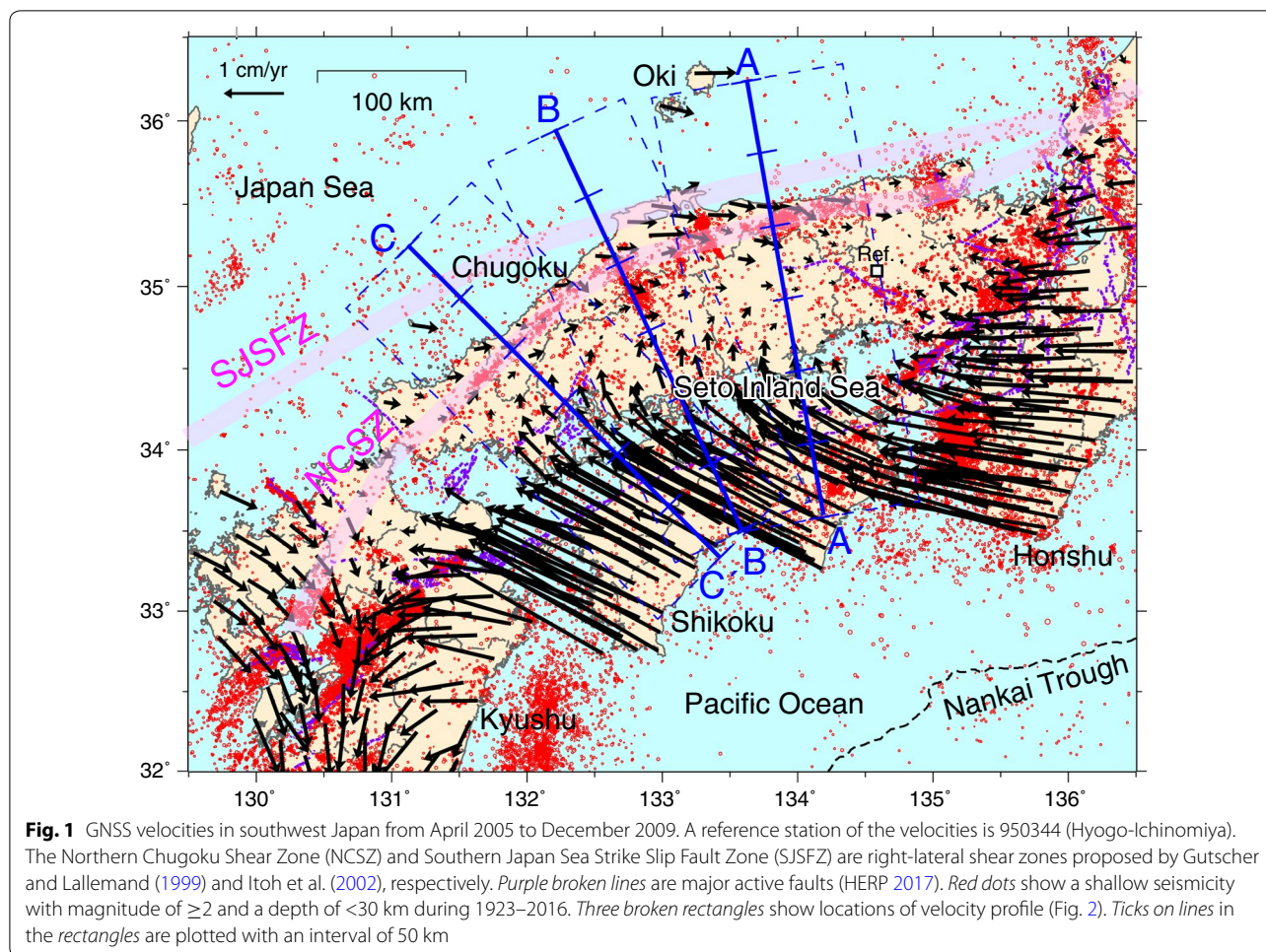which is the northern part of westernmost Honshu facing the Japan Sea.

Although shallow historical large earthquakes and microseismicity show a clear lineaments along the coastline (Gutscher 2001; Kawanishi et al. 2009), no major active faults have been identified in the San-in region (HERP 2017). A detailed geomorphological study suggests that ENE–WSW trending dextral active faults and NNW–SSE trending sinistral ones are distributed in the San-in region, but that they are young developing faults with cumulative offsets of less than a few hundreds of meters (Okada 2002).

Owing to a nationwide GNSS network installed in mid 1990s, contemporary deformation of the Japanese Islands is monitored in detail. Sagiya et al. (2000) analyzed the GNSS data and found a concentrated region of strain rates far from major plate boundaries including the Nankai Trough and Japan Trench in central Japan. However, they did not identify concentration of strain rates in the San-in region. Loveless and Meade (2010) studied the GEONET data to clarify velocity profile across the NCSZ

*Correspondence: nishimura.takuya.4s@kyoto-u.ac.jp
[1] Disaster Prevention Research Institute, Kyoto University, Uji 611-0011, Japan
Full list of author information is available at the end of the article

**Fig. 1** GNSS velocities in southwest Japan from April 2005 to December 2009. A reference station of the velocities is 950344 (Hyogo-Ichinomiya). The Northern Chugoku Shear Zone (NCSZ) and Southern Japan Sea Strike Slip Fault Zone (SJSFZ) are right-lateral shear zones proposed by Gutscher and Lallemand (1999) and Itoh et al. (2002), respectively. *Purple broken lines* are major active faults (HERP 2017). *Red dots* show a shallow seismicity with magnitude of ≥2 and a depth of <30 km during 1923–2016. *Three broken rectangles* show locations of velocity profile (Fig. 2). *Ticks on lines* in the *rectangles* are plotted with an interval of 50 km

and construct the block model of the Japan region. They showed ≤3 mm/year of right-lateral slip rates along the NCSZ in the block model but no significant relative motion in the velocity profile across the NCSZ. They, therefore, concluded that the NCSZ does not play an important role in the larger-scale tectonics of Western Honshu. No other geodetic studies have pointed out right-lateral movements in the San-in region.
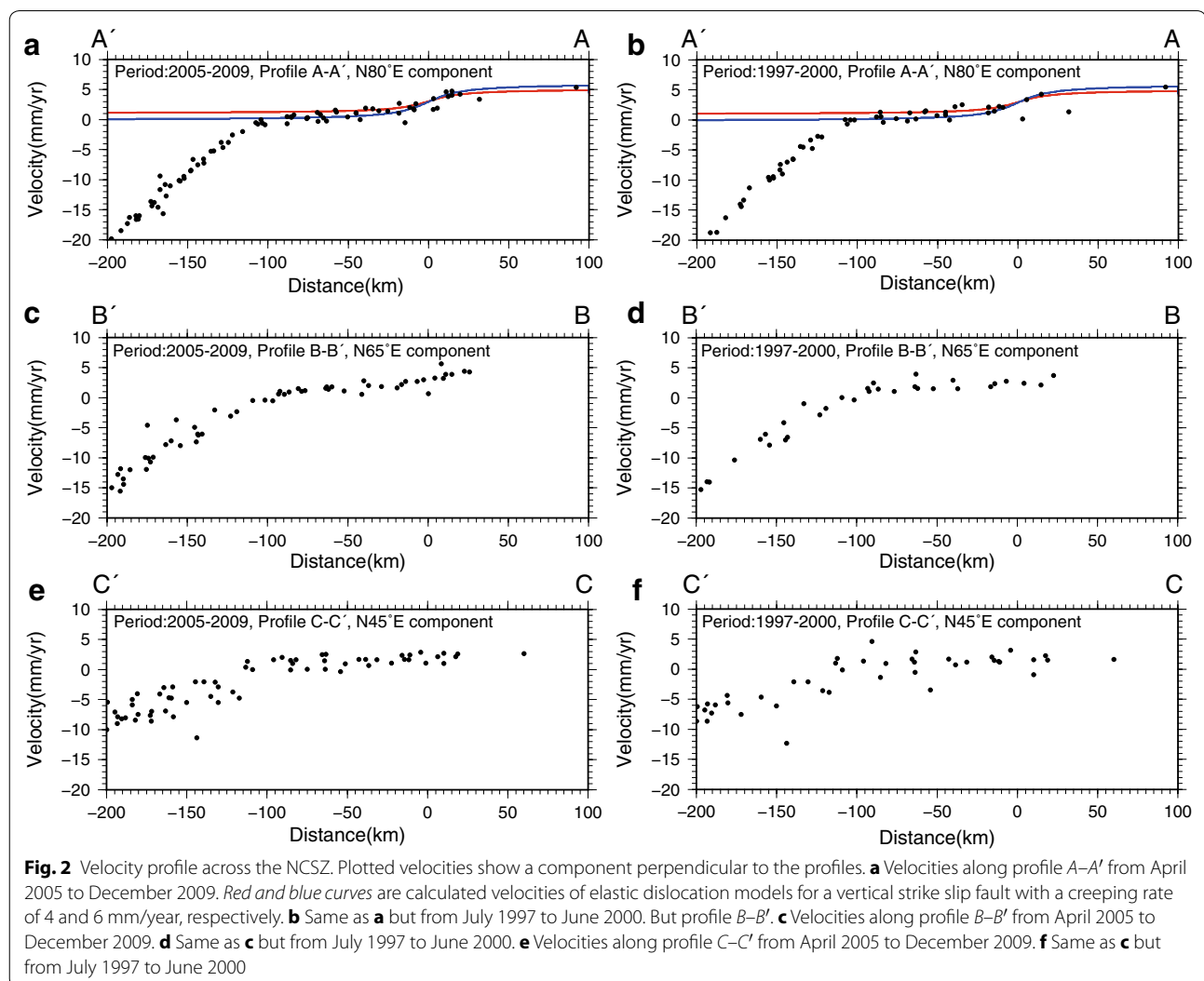
Several large earthquakes including the 2000 $M_{\mathrm{JMA}}$ (magnitude determined by the Japan Meteorological Agency) 7.3 western Tottori earthquake and the 2016 $M_{\mathrm{JMA}}$6.6 central Tottori earthquake occurred in the San-in region, which means that the region is seismotectonically active. However, GNSS data in the region have not been fully examined although the number of GNSS stations has been increased by ~50% in the twenty-first century. In this paper, we examine a dense GNSS data to clarify whether significant movements are ongoing in the San-in regions and model the movements with a simple dislocation model. We also discuss a distribution of microseismicity in a shear zone.

## GNSS velocity data

We use data of continuous GNSS stations of the GNSS Earth Observation Network System (GEONET) (cf. Sagiya et al. 2000). We estimate secular GNSS velocities in a period from April 2005 to December 2009. There were no earthquakes and slow slip events causing significant crustal deformation in southwest Japan during this period. The velocities are estimated by fitting linear, annual, and semiannual terms to daily coordinates of the GEONET F3 solution (Nakagawa et al. 2009). Uncertainties of the horizontal velocities assuming a white noise model are 0.02–0.05 mm/year. Although these values can be underestimated by an order because the noise characteristics of GNSS time series are time-correlated (e.g., Mao et al. 1999), velocity errors are so small that we can ignore the data errors in the following analysis. Figure 1 shows horizontal velocities with respect to the 950344 station. We remove several vectors at anomalous stations which are inconsistent with velocities at surrounding stations. We found monuments of the anomalous stations are mostly inclined by visual inspection. Although

the most distinctive feature of Fig. 1 is velocities toward WNW along the Pacific coast, which is caused by inter-plate coupling between the subducting Philippine Sea and the overriding Amurian plates (e.g., Yoshioka and Matsuoka 2013), eastward velocities along the coast-line of the Japan Sea between ~132.5°E and ~135°E are recognized with respect to the reference station. These eastward velocities are small in the southern side of the NCSZ corresponding to a zone of active shallow micro-seismicity. Deformation rates across the NCSZ are clari-fied by projections of velocity profiles. Figure 2a–c shows velocity profiles along sections *A−A′*, *B−B′*, and *C−C′* across the NCSZ shown in Fig. 1, respectively. Veloc-ity components shown in Fig. 2a–c are N80°E, N65°E, and N45°E components perpendicular to the sections, respectively. Along section *A−A′* (Fig. 2a), distinctive velocity gradient in a distance of ≤−100 km is mainly

attributed to elastic deformation due to interplate cou-pling along the Nankai Trough. Velocities between −100 and −30 km are almost constant, which means lower deformation rates between the Seto Inland Sea and Chu-goku Mountains. We identify steep velocity gradient around a distance of 0 km. The velocities there shift from ~1 to ~4 mm/year with a transition width of ~50 km. No significant difference of velocities between the coastline of Japan Sea (distance ~30 km) and Oki Island (distance ~90 km). On the other hand, no significant gradients in velocities are recognized in a distance between −100 and 100 km along section *C−C′*. Along section *B−B′*, gradient is recognized around a distance of 0 km and gentler than that along *A−A′*. Because there are no clear gradients of velocity components parallel to the sections around a distance of 0 km either, the contemporary deformation is concentrated only in an eastern part of the NCSZ. The



**Fig. 2** Velocity profile across the NCSZ. Plotted velocities show a component perpendicular to the profiles. **a** Velocities along profile *A−A′* from April 2005 to December 2009. *Red and blue curves* are calculated velocities of elastic dislocation models for a vertical strike slip fault with a creeping rate of 4 and 6 mm/year, respectively. **b** Same as **a** but from July 1997 to June 2000. But profile *B−B′*. **c** Velocities along profile *B−B′* from April 2005 to December 2009. **d** Same as **c** but from July 1997 to June 2000. **e** Velocities along profile *C−C′* from April 2005 to December 2009. **f** Same as **c** but from July 1997 to June 2000

analysis of strain rates (Nishimura et al., submitted manuscript) also suggests that high strain rates are concentrated along the NCSZ between 132.7°E and 135.2°E. We propose to call this concentrated deformation zone as the San-in shear zone (SSZ).
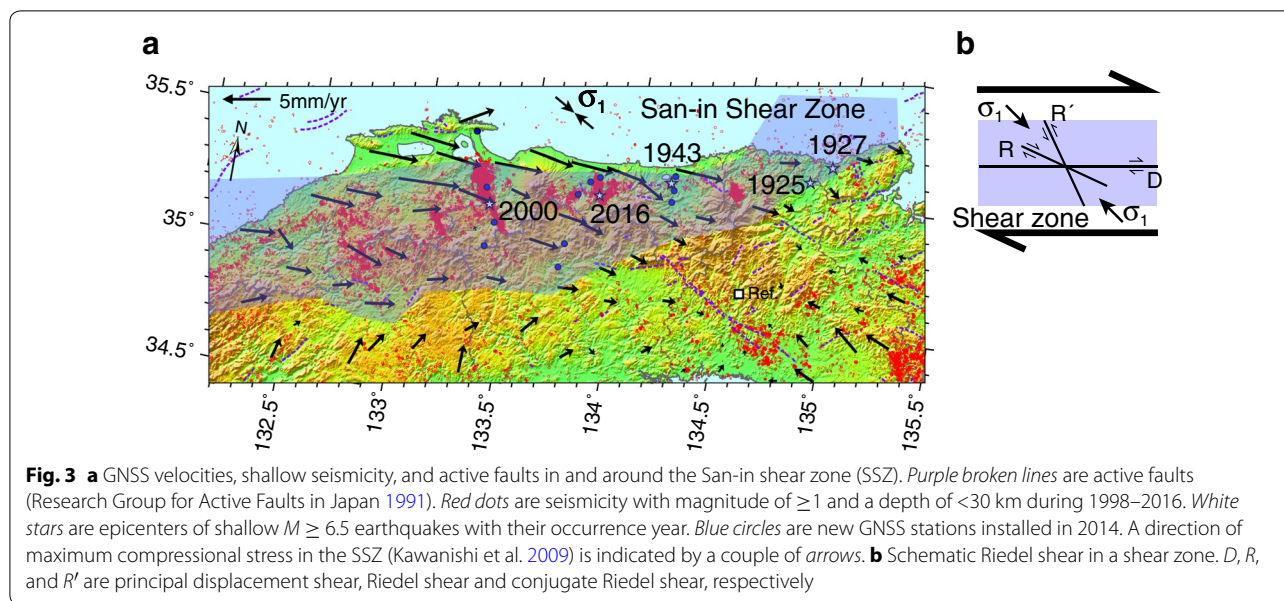
## Deformation modeling and discussion

High velocity gradients can be explained by a simple elastic dislocation model. We assume a two-dimensional vertical fault with right-lateral strike slip. The fault is locked from surface to a locking depth and creeps below the locking depth to infinity. The surface velocity parallel to the fault with an elastic half-space is a symmetric pattern of arctangent with respect to the fault (Savage and Burford 1973). The calculated velocities are shown by red and blue curves with a creeping rate of 4 and 6 mm/year and a locking depth of 16 km (Fig. 2a). The calculated velocities roughly reproduce the observed ones around a distance of 0 km. Least square fitting for the data at a distance between −100 and 100 km suggests $6.4 \pm 1.0$ mm/year and $28 \pm 10$ km for a creeping rate and a locking depth, respectively, but the estimated creeping rate may be an upper bound due to ignoring other deformation sources including interplate coupling along the Nankai Trough. The estimated locking depth is significantly deeper than a cutoff depth of crustal seismicity (~10 km) (Omuralieva et al. 2012), but it must be affected by ignoring variations of the locking depth and fault geometry along the SSZ. Although it is difficult to resolve these problems from the limited sparse GNSS data, a comparison between the observed and calculated velocities suggests the right-lateral strike movements beneath a locking depth at a rate of ~5 mm/year along the SSZ.

Another possibility to cause strain rate concentration in the SSZ is postseismic deformation of recent large earthquakes including the 1927 $M_{JMA}$7.3 Tango, the 1943 $M_{JMA}$7.2 Tottori, and the 2000 $M_{JMA}$7.3 western Tottori earthquake. Viscoelastic relaxation of a large earthquake generally continues for more than several decades. We use a layered viscoelastic half-space model (Wang et al. 2006) to calculate postseismic deformation due to viscoelastic relaxation with varying Maxwell viscosities of upper mantle and lower crust. If viscosities of upper mantle and lower crust are, respectively, assumed to be $5 \times 10^{18}$ and $5 \times 10^{19}$ Pa s which are estimated from postseismic deformation of the 1927 Tango earthquake (Tabei 1989), surface velocity in 2005 is less than 1.3 mm/year. If we assume viscoelastic lower crust is an order of $10^{19}$ Pa s, the strain rate concentration near the SSZ can be reproduced qualitatively. However, the viscoelastic model cannot reproduce observed eastward velocity in an area a 1000 km north of the SSZ because a scale of deformation due to calculated viscoelastic relaxation

is less than a few 100 km. The observed velocity in the remote area including Korean Peninsula and the China continent is eastward and similar to that on Oki Island (Nishimura et al. submitted manuscript), which can be regarded as a rigid block motion north of the SSA. We, therefore, conclude that postseismic deformation is not a main cause of ongoing deformation in the SSZ.

The apparent concentration of strain rates along the SSZ makes us to question why previous GNSS studies did not notice the SSZ. Loveless and Meade (2010) examined velocities around the NCSZ and found no significant deformation. We suggest two possibilities for apparent difference. First, concentration of strain rates is observed only in the SSZ, not all over the NCSZ. Second, distribution of GNSS stations before 2002 is not enough to detect concentration of strain rates in the SSZ. We plot velocity profiles along sections $A–A'$, $B–B'$, and $C–C'$ during July 1997–June 2000 (Fig. 2b, d, f). A velocity gradient is unclear at a distance of 0 km along sections $A–A'$ because few stations locate north of the SSZ (Fig. 2b). After 2002, several new stations have been installed and some stations showing local deformation have been replaced around the SSZ. Therefore, it is clear in the velocity profile after 2005 (Fig. 2a). Because of no velocity change on Oki Island (around a distance of 90 km in Fig. 2a, b), the apparent temporal change of the velocity profile is probably caused by artificial redistribution of the GNSS network.

The SSZ is generally oriented in an azimuth of N70–80°E along the coastline, and the observed velocities are well explained by right-lateral strike slip movements of the SSZ as explained in the previous section. However, each cluster of microseismicity within the SSZ is oriented in NNW–SSE (Fig. 3) and finite fault models for recent large earthquakes (cf. Nishida 1990; Sagiya et al. 2002) also suggest left-lateral strike slip on faults whose strike is NNW–SSE, except for the 1943 Tottori earthquake (Kanamori 1972) whose strike is N80°E with right-lateral strike slip. We propose that the NNW–SSE faulting is conjugate Riedel shears in a shear zone (Fig. 3). Numerous cracks and structures in addition to principal displacement shears develop in a shear zone with a scale from a shear experiment in laboratory to surface rupture in field (cf. Tchalenko 1970). The formation of Riedel shears and conjugate Riedel shears is explained by fracture planes under maximum compressional stress in the shear zone with the Mohr–Coulomb failure criterion. The maximum compressional stress estimated from focal mechanisms of earthquakes in the San-in shear zone (Kawanishi et al. 2009) lies with an angle of ~45° with respect to the orientation of the shear zone (Fig. 3). Conjugate Riedel shears develop at an early stage of the shear zone formation according to the laboratory experiments (Tchalenko

**Fig. 3** **a** GNSS velocities, shallow seismicity, and active faults in and around the San-in shear zone (SSZ). *Purple broken lines* are active faults (Research Group for Active Faults in Japan 1991). *Red dots* are seismicity with magnitude of $\geq 1$ and a depth of <30 km during 1998–2016. *White stars* are epicenters of shallow $M \geq 6.5$ earthquakes with their occurrence year. *Blue circles* are new GNSS stations installed in 2014. A direction of maximum compressional stress in the SSZ (Kawanishi et al. 2009) is indicated by a couple of *arrows*. **b** Schematic Riedel shear in a shear zone. *D*, *R*, and *R′* are principal displacement shear, Riedel shear and conjugate Riedel shear, respectively

1970). There are no single active faults regarded as a principal displacement shear but young active faults with a strike of ENE–WSW or NNW–SSE in the SSZ (Okada 2002). These manifest that the SSZ is a young and developing shear zone in a geological time scale.

The SSZ locates along a volcanic front of the subducting Philippine Sea plate. Low velocity of seismic waves in upper mantle beneath the SSZ and a high $^3$He/$^4$He ratio suggest upwelling fluid from the mantle in the SSZ (Nakajima and Hasegawa, 2007; Sano and Nakajima 2008). These observations suggest that the fluid weaken the lower crust (i.e., Iio et al. 2002). High temperature induced from high heat flow (Tanaka et al. 2004) and the shallow cutoff depth of seismicity (Omuralieva et al. 2012) also contribute to weaken the lower crust in the SSZ. Oblique subduction of the Philippine Sea can drive the aseismic faulting or ductile flow in the weakened lower crust examined by Kawanishi et al. (2009) and this study. We propose that the SSZ is a shear zone for strain partitioning within the continental plate and accommodates a part of relative motion between the subducting Philippine Sea and the overriding continental plates, as suggested by previous studies (Tsukuda 1992; Gutscher and Lallemand 1999; Gutscher 2001). Although the concentration zone of strain rates observed by GNSS is limited between 132.7°E and 135.2°E, similar movements probably extend to east and west. Because we do not identify the concentrated deformation in eastern and western extensions on land, we speculate that right-lateral strike slip movements are more diffusive in the extensions and are accommodated mainly in an offshore region.

We constructed 13 continuous GNSS stations across the SSZ to clarify a detailed deformation in and around the SSZ in 2014 as denoted by blue circles in Fig. 3. These stations observed near field co- and postseismic displacement of the $M_{\text{JMA}}$ 6.6 central Tottori earthquake occurred in October 21, 2016. A further analysis including these data on the SSZ will be presented in near future.

## Conclusions

We analyzed GNSS data in southwest Japan and found a concentrated deformation zone along the coastline of the Japan Sea between 132.5°E and 135°E. This zone is a part of the Northern Chugoku Shear Zone based on a seismological and geological study (Gutscher and Lallemand 1999). This study has first identified the concentrated shear zone in the San-in area geodetically, and we propose to call the concentrated deformation zone the San-in shear zone (SSZ), which accommodates a right-lateral strike slip movement with a width of ~50 km. A simple dislocation model of vertical dextral fault with a shallow locking and a deep creeping of ~5 mm/year reproduces the observed velocity pattern across the SSZ. Although the SSZ is characterized by active shallow microseismicity, each cluster of microseismicity and faults ruptured by recent large earthquakes are almost oriented in NNW–SSE which is oblique to the overall trend of the SSZ. We propose the oblique seismicity is attributed to conjugate Riedel shears in a young developing shear zone. From the view point of regional tectonics, it is proposed that the SSZ is a shear zone for strain partitioning within the southern margin of the continental Amurian plate and accommodates a part of relative motion of the subducting Philippine Sea plate.

## Author details
[1] Disaster Prevention Research Institute, Kyoto University, Uji 611-0011, Japan. [2] Graduate School of Science, Hokkaido University, Sapporo 060-0810, Japan.

## Publisher's Note
Springer Nature remains neutral with regard to jurisdictional claims in published maps and institutional affiliations.

## References
Gutscher MA (2001) An Andean model of interplate coupling and strain partitioning applied to the flat subduction zone of SW Japan (Nankai Trough). Tectonophysics 333:95–109. doi:10.1016/S0040-1951(00)00269-9
Gutscher MA, Lallemand S (1999) Birth of a major strike-slip fault in SW Japan. Terra Nova 11:203–209. doi:10.1046/j.1365-3121.1999.00247.x
Headquarters for Earthquake Research Promotion (HERP) (2017) Evaluations of active faults. http://www.jishin.go.jp/evaluation/long_term_evaluation/major_active_fault/. Accessed 30 Mar 2017 (in Japanese)
Iio Y, Sagiya T, Kobayashi Y, Shiozaki I (2002) Water-weakened lower crust and its role in the concentrated deformation in the Japanese Islands. Earth Planet Sci Lett 203:245–253
Itoh Y, Tsutsumi H, Yamamoto H, Arato H (2002) Active right-lateral strike-slip fault zone along the southern margin of the Japan Sea. Tectonophysics 351:301–314. doi:10.1016/S0040-1951(02)00164-6
Kanamori H (1972) Determination of effective tectonic stress associated with earthquake faulting. The Tottori earthquake of 1943. Phys Earth Planet Inter 5:426–434
Kawanishi R, Iio Y, Yukutake Y, Shibutani T, Katao H (2009) Local stress concentration in the seismic belt along the Japan Sea coast inferred from precise focal mechanisms: implications for the stress accumulation process on intraplate earthquake faults. J Geophys Res 114:B01309. doi:10.1029/2008JB005765
Loveless JP, Meade BJ (2010) Geodetic imaging of plate motions, slip rates, and partitioning of deformation in Japan. J Geophys Res 115:B02410. doi:10.1029/2008JB006248
Mao A, Harrison CGA, Dixon TH (1999) Noise in GPS coordinate time series. J Geophys Res 104:2797–2816. doi:10.1029/1998JB900033
Nakagawa H, Toyofuku T, Kotani K, Miyahara B, Iwashita C, Kawamoto S, Hatanaka Y, Munekane H, Ishimoto M, Yutsudo T, Ishikura N, Sugawara Y (2009) Development and validation of GEONET new analysis strategy (Version 4). J Geogr Surv Inst 118:1–8 (in Japanese)
Nakajima J, Hasegawa A (2007) Tomographic evidence for the mantle upwelling beneath southwestern Japan and its implications for arc magmatism. Earth Planet Sci Lett 254:90–105
Nishida R (1990) Characteristics of the 1983 Tottori earthquake sequence and its relation to the tectonic stress field. Tectonophysics 174:257–278. doi:10.1016/0040-1951(90)90325-3
Okada A (2002) Characteristics of the active faults in the San'in district, western Japan. Active Fault Res 22:17–32 (in Japanese with English abstract)
Omuralieva AM, Hasegawa A, Matsuzawa T, Nakajima J, Okada T (2012) Lateral variation of the cutoff depth of shallow earthquakes beneath the Japan Islands and its implications for seismogenesis. Tectonophysics 518:93–105. doi:10.1016/j.tecto.2011.11.013
Research Group for Active Faults of Japan (1991) Active Faults in Japan: Sheet Maps and Inventories, revised edn. University of Tokyo Press, Tokyo (in Japanese with English summary)
Sagiya T, Miyazaki S, Tada T (2000) Continuous GPS array and present-day crustal deformation of Japan. Pure Appl Geophys 157:2302–2322. doi:10.1007/PL00022507
Sagiya T, Nishimura T, Hatanaka Y (2002) Crustal movements associated with the 2000 Western Tottori earthquake and its fault models. J Seismol Soc Jpn 54:523–534 (in Japanese with English abstract)
Sano Y, Nakajima J (2008) Geographical distribution of $^3$He/$^4$He ratios and seismic tomography in Japan. Geochem J 42:51–60
Savage JC, Burford RO (1973) Geodetic determination of relative plate motion in central California. J Geophys Res 78:832–845. doi:10.1029/JB078i005p00832
Tabei T (1989) Crustal movements in the inner zone of southwest Japan associated with stress relaxation after major earthquakes. J Phys Earth 37:101–131
Tanaka A, Yamano M, Yano Y, Sasada M (2004) Geothermal gradient and heat flow data in and around Japan (I). Earth Planets Space 56:1191–1194. doi:10.1186/BF03353339
Tchalenko JS (1970) Similarities between shear zones of different magnitudes. Geol Soc Am Bull 81:1625–1640
Tsukuda E (1992) Active tectonics of Southwest Japan arc controlled by the westward translation of the forearc sliver (in Japanese with English abstract). Mem Geol Soc Jpn 40:235–250
Wang R, Lorenzo-Martín F, Roth F (2006) PSGRN/PSCMP—a new code for calculating co-and post-seismic deformation, geoid and gravity changes based on the viscoelastic-gravitational dislocation theory. Comput Geosci 32:527–541
Yoshioka S, Matsuoka Y (2013) Interplate coupling along the Nankai Trough, southwest Japan, inferred from inversion analyses of GPS data: effects of subducting plate geometry and spacing of hypothetical ocean-bottom GPS stations. Tectonophysics 600:165–174. doi:10.1016/j.tecto.2013.01.023